HHS Public Access

Author manuscript

Nat Immunol. Author manuscript; available in PMC 2009 November 01.

Published in final edited form as:

Nat Immunol. 2009 May ; 10(5): 504–513. doi:10.1038/ni.1729.

Foxo3 controls the magnitude of T cell immune responses by modulating dendritic cell function

Anne S. Dejean[1], **Daniel R. Beisner**[1,2], **Irene L. Ch'en**[1], **Yann M. Kerdiles**[1], **Anna Babour**[1], **Karen C. Arden**[3], **Diego H. Castrillon**[4,5], **Ronald A. DePinho**[4], and **Stephen M. Hedrick**[1]

[1]Molecular Biology Section, Division of Biological Sciences, and Department of Cellular and Molecular Medicine, University of California, San Diego 92093-0377

[3]Ludwig Institute for Cancer Research, University of California, San Diego School of Medicine, La Jolla, CA 92093-0660

[4]Center for Applied Cancer Science, Belfer Institute for Innovative Cancer Science, Departments of Adult Oncology, Medicine and Genetics, Dana-Farber Cancer Institute, Harvard Medical School, Boston, MA 02115

Abstract

Foxo transcription factors regulate cell cycle progression, survival, and DNA repair pathways. Here, we demonstrate that a deficiency in Foxo3 resulted in increased expansion of T cell populations after viral infection. This exaggerated expansion was not T cell intrinsic. Rather, it was caused by the enhanced capacity of Foxo3-deficient dendritic cells to sustain T cell viability by producing increased amounts of interleukin 6 (IL-6). CTLA-4-mediated stimulation of dendritic cells induced nuclear localization of Foxo3, which in turn inhibited IL-6 and tumor necrosis factor production. Thus, Foxo3 acts to constrain dendritic cell production of key inflammatory cytokines and control T cell survival.

Introduction

Foxo transcription factors guide the cellular response to growth factors, nutrients and stress. This information is encoded as post-translational modifications—referred to as a 'Foxo code'—that govern Foxo intracellular localization, cofactor associations, and transcriptional activity. The resulting program of gene expression regulates cell cycle arrest, repair, apoptosis, autophagy, and many other aspects of cellular homeostasis1. In mammals, four

Correspondence to: Stephen M Hedrick[1], e-mail: shedrick@ucsd.edu.

[2]Present address: Genetics Institute of the Novartis Foundation, 10675 John Jay Hopkins Drive, San Diego CA 92121

[5]Present address: Department of Pathology, UT Southwestern Medical Center at Dallas, 5323 Harry Hines Blvd, Dallas, Texas 75390-9072

Author contributions: D.R.B. initiated the project and conducted the lymphocyte characterization and LCMV infection under the supervision of S.M.H. A.S.D. designed and conducted the remaining experiments in collaboration with D.R.B., I.L.C., Y.M.K. and S.M.H. A.B. provided essential expertise in the fluorescence microscopy analysis. R.A.D. and D.H.C. produced the *Foxo3*$^{-/-}$ mice and provided intellectual input on the data presented in the manuscript. K.C.A. provided the *Foxo3*^{Kca} mice. S.M.H. initiated the project with input from R.A.D. and K.C.A., and supervised the experimentation. A.S.D. and S.M.H. wrote the manuscript with editorial and intellectual contributions from the other authors.

Foxo members have been identified. Foxo1 (FKH1, FKHR)2, Foxo3 (FKHRL1) (http://www.signaling-gateway.org/molecule/query?afcsid=A000945)3, and Foxo4 (AFX)4 are widely expressed and similarly regulated, whereas and Foxo65 expression is confined to specific structures of the brain and is subject to distinct regulatory mechanisms.

Insulin, insulin-like growth factor, and other growth factors induce activation of PI3 kinase and Akt, which phosphorylate three Foxo amino acids6. These modifications result in Foxo association with the adaptor protein 14-3-3, and Foxo3 nuclear exclusion and eventual degradation7–9. This process can be actively opposed by stress-induced signals that activate the Jnk MAP kinase, which result in Foxo3 nuclear localization10. Foxo factor target specificity can be further refined by the SIRT1 deacetylase11,12.

Given its role in coordinating cellular growth, proliferation, and survival, we predicted that Foxo factors would be central to the highly dynamic, infection-mediated expansion and contraction of antigen-specific T cell populations. Indeed, Foxo activity is regulated by T cell receptor (TCR) and CD28 signaling, as well as by cytokines such as interleukin 2 (IL-2)13, IL-314, and IL-715,16. These stimuli result in the phosphorylation of Foxo by Akt, serum/glucocorticoid-regulated kinase (Sgk) or IκB kinase (IKK), and in nuclear exclusion of Foxo317. Growth factor withdrawal causes dephosphorylation of nuclear Foxo3, binding of Foxo3 to the Bim and Puma promoters, induction of Bim and Puma transcription, and T cell apoptosis18. In contrast, enforced expression of a constitutively nuclear form of Foxo3 in T cell lines caused cell cycle arrest13. Furthermore, Foxo3 plays a role in the persistence of $CD4^+$ central memory T cells in mice and humans19.

Previous studies utilizing a mutant allele generated by ‘gene-trap’ technology ($Foxo3^{Trap}$) revealed spontaneous T cell activation, lymphoproliferative disease, and organ infiltration20. These studies point to an important role of Foxo3 in immune regulation, although the underlying molecular mechanisms are not understood. In addition, Foxo3 regulates superoxide dismutase in dendritic cells (DC); this signaling pathway may affect the production of suppressive or stimulating characteristics of plasmacytoid DCs21,22.

In this study, we sought to determine whether Foxo3 plays a role in immune cell quiescence and the dynamics of T cell expansion and contraction. We found that, in response to LCMV infection, Foxo3 deficiency caused superabundant expansion of antigen-specific T cell populations. However, contrary to our expectations, this phenotype was not intrinsic to T cells, but rather, it arose from altered stimulatory properties of Foxo3-deficient DCs. Foxo3 deficiency resulted in a DC-specific increase in the production of IL-6. Foxo3 nuclear localization induced by signals initiated by cytotoxic T lymphocyte-associated antigen 4 (CTLA-4) (http://www.signaling-gateway.org/molecule/query?afcsid=A000706) suppressed Toll-like receptor (TLR)-induced IL-6 production. Together, these studies highlight the importance of Foxo3 in restraining DC inflammatory cytokine production and T cell viability.

RESULTS

No spontaneous activation of Foxo3-deficient T cells

To examine the role of Foxo3 in the immune system, we utilized two independently derived *Foxo3*-null strains distinct from the *Foxo3*^{Trap} mutant20. One strain, referred to as *Foxo3*^{Kca}, was backcrossed to the C57BL/6 strain whereas the other, referred to as *Foxo3*$^{-/-}$, was maintained as congenic FVB mice. Although strain-specific differences were detected, Foxo3 deletion had no impact on the proportion of T or B cells in the spleen and lymph nodes (LN) of 6–10 week old mice (Table 1). However, we noted an increased proportion of Gr-1^{hi}CD11b^{hi} cells, which include granulocytes and macrophages, in the spleens of both Foxo3-deficient strains. We detected neither lymphocytic organ infiltration nor lymphadenopathy (data not shown)23 in 6–10 week old Foxo3-deficient mice. However 3–6 month old Foxo3-deficient mice showed an enlargement of the spleen and an increase in erythrocyte progenitors (Ter119^{+}) (data not shown). This observation likely relates to the previously characterized decrease in erythrocyte lifespan and the rate of erythrocyte maturation in Foxo3-deficient mice24. Next we measured the expression of CD69, CD44 and CD62L (L-selectin) on T cells in Foxo3-deficient and wild-type littermate mice. Whereas we again detected differences between C57BL/6 and FVB strains, inactivation of *Foxo3* had no impact on the proportion of activated (CD69^{hi}) or memory-effector (CD44^{hi}CD62L^{lo}) T cells (Fig. 1a).

Previous studies revealed a constitutive activation of the NF-κB pathway in *Foxo3*^{Trap} mice, as reflected by the absence of IκB20. However, T cells purified from *Foxo3*$^{Kca/Kca}$ and *Foxo3*$^{-/-}$ mice showed no changes in the expression of IκBα, IκBβ, and IκBεε proteins (Supplementary Fig. 1, online). To measure the effect of Foxo3 deficiency on T cell proliferation, purified LN T cells were labeled with carboxyfluorescein diacetate succinimidyl ester (CFSE), and cultured with plate-bound anti-CD3 with or without anti-CD28. Neither the number of cell divisions nor the accumulation of cells in each division was altered by Foxo3 deficiency (Fig. 1b). In addition, freshly explanted *Foxo3*$^{Kca/Kca}$ and wild-type CD4 and CD8 T cells produced similar amounts of cytokines (Fig. 1c). As FasL is a known target of Foxo3, we also analyzed the expression of FasL on unstimulated or stimulated T cells from wild-type and *Foxo3*$^{Kca/Kca}$ mice; however we found no differences associated with Foxo3 status (data not shown). These results suggest that loss of Foxo3 alone is not sufficient to provoke manifestations of T cell activation and spontaneous autoimmunity.

Foxo3$^{Kca/Kca}$ mice exhibit enhanced T cell accumulation

As Foxo3 plays a role in cell cycle progression and apoptosis25, we sought to investigate its role in the dynamics of T cell population expansion and contraction in response to viral infection. Historically, the C57BL/6 strain has been used to study the progression of viral responses, and, as the two Foxo3 homozygous mutant strains showed identical profiles here and previously23,26, our further characterization efforts focused on C57BL/6 *Foxo3*$^{Kca/Kca}$ mice (referred to as *Foxo3*^{Kca}).

Foxo3^{Kca} mice and wild-type littermates were infected with lymphocytic choriomeningitis virus (LCMV), and LCMV-responsive T cell populations were enumerated at various days post-infection. Whereas the *Foxo3* genotype had no impact on the kinetics of T cell population expansion, *Foxo3*^{Kca} mice developed a 3-fold greater accumulation of LCMV-specific T cells compared to wild-type littermates (Fig. 2). A measurement of virus in the livers of mice at day 8 post-infection revealed complete viral clearance in both strains (data not shown).

The lack of an effect of Foxo3 deficiency on T cells stimulated in culture prompted us to test whether the enhanced T cell accumulation during an LCMV response was T cell-intrinsic. To this end, we transferred T cells from LCMV-specific TCR transgenic P14 *Foxo3*^{Kca} or P14 wild-type mice into wild-type C57BL/6 mice, and measured the accumulation of P14 T cells after infection of recipient mice with LCMV. We detected no significant differences in the accumulation of *Foxo3*^{Kca} versus wild-type P14 T cells (Fig. 2b). To further examine this issue, wild-type P14 T cells were transferred into either wild-type or *Foxo3*^{Kca} mice, and recipients were infected with LCMV. P14 T cells transferred into *Foxo3*^{Kca} accumulated in greater numbers than P14 T cells transferred into wild-type hosts (Fig. 2b). This result was reproduced with the transfer of OVA-specific OTI T cells into wild-type and *Foxo3*^{Kca} hosts that were subsequently infected with OVA-expressing vesicular stomatitis virus (VSV) (Supplementary Fig. 2, online).

To further examine the cellular cause of the exaggerated T cell population expansion, irradiated wild-type mice were reconstituted with bone marrow (BM) from either wild-type or *Foxo3*^{Kca} mice. After 8 weeks, recipient mice were infected with LCMV and the expansion of LCMV-specific T cell population was analyzed. Excessive T cell accumulation was apparent in recipients of *Foxo3*^{Kca} BM, implicating BM-derived cell type(s) in this phenotype (Fig. 2c). Thus, a non-T cell BM-derived cell type(s) is responsible for the enhanced T cell proliferation and/or survival observed in Foxo3-deficient mice.

Stimulatory capacity of DCs in *Foxo3*^{Kca} mice

The efficiency of antigen presentation can affect the magnitude of a T cell response to viral infection27. As such, we tested whether Foxo3 regulates the number, phenotype and/or function of antigen presenting DCs. The number of DCs in naïve *Foxo3*^{Kca} mice relative to wild-type littermates was significantly increased (Fig. 3a), and there was a small increase in the proportion of DCs that expressed high amounts of B7-1 and B7-2. No change was noted for MHC class I, MHC class II, or CD40 expression on DCs (Fig.3b), suggesting that a small number of Foxo3 -deficient DCs exhibited a more mature phenotype.

An analysis of different DC subsets showed increased numbers of $CD11c^+CD11b^+CD8^-$, $CD11c^+CD11b^-CD8^+$ and $CD11c^+B220^+$ DCs in Foxo3-deficient mice (Fig. 3c). All subsets exhibited a moderate shift toward high expression of B7-1 and B7-2 (Fig. 3d), although the biological importance of this shift is unclear. To further characterize the activation status of DCs from naïve mice, splenic DCs were placed into culture overnight, and secreted cytokines were measured. *Foxo3*^{Kca} DCs produced more IL-6, TNF, and MCP-1 than wild-type DCs (Fig 3e). IFN-γ, IL-10, and IL-12 were undetectable (data not shown).

To determine whether DCs from *Foxo3*^{Kca} mice exhibit enhanced antigen presentation, mice were infected with LCMV, and DCs were analyzed 3 days after infection, when virus is still present and T cell populations are exponentially expanding28. Compared to wild-type DCs, *Foxo3*^{Kca} DCs expressed slightly higher amounts of B7-1, B7-2 and MHC class II (Fig. 4a), and more effectively stimulated P14 T cell accumulation as measured by CFSE dilution and Annexin V versus 7-AAD staining (Fig. 4b). This enhanced stimulatory capacity was not due to a difference in antigen processing, as differences between cultures with *Foxo3*^{Kca} and wild-type DCs remained even after DCs were pulsed with LCMV gp33 peptide (Fig. 4b).

To rule out the possibility that Foxo3-deficient DCs from LCMV-infected mice can cause bystander T cell proliferation independent of the presence of antigen, DCs from LCMV-infected mice were also cultured with OTI T cells with or without OVA peptide. Ruling out the possibility of bystander effects, in the absence of OVA peptide, there was no detectable OTI T cell division (Fig. 4b). Finally, we measured the capacity of DCs from uninfected mice to stimulate P14 T cells in the presence of gp33 peptide. We noted a modest increase in the accumulation and viability of T cells from cultures containing *Foxo3*^{Kca} compared to wild-type DCs (Fig. 4c).

To determine if the enhanced function of Foxo3-deficient DCs is cell-autonomous, we generated DCs *in vitro*. To this end we cultured bone marrow (BM) cells for 8 days with GM-CSF. The number and proportion of the resulting CD11c^{+} cells (referred to as BMDCs) were unaffected by Foxo3 status, and none of the BMDCs showed elevated expression of B7-1, B7-2, CD40, MHC class I, or MHC class II (Supplementary Fig. 3a, online). Consistent with previous reports of GM-CSF-stimulated cells, wild-type BMDCs displayed a uniform Foxo3 cytoplasmic localization29 (Supplementary Fig. 3b, online). Next we used BMDCs to stimulate OTII and P14 T cells at various ratios of T cells to DCs. Compared with wild-type BMDCs, *Foxo3*^{Kca} BMDCs more effectively induced accumulation of OTII and P14 T cells (Fig. 5a). Moreover, the Foxo3-deficient BMDCs also more effectively sustained T cell viability, irrespective of cell division (Fig. 5b,c). To determine whether the differences in viability correlate with changes in Bcl-2 family members, we analyzed the expression of Bcl-2 and Bcl-xL. Total and naïve CD44^{lo} T cells expressed higher amounts of both pro-survival factors when stimulated with Foxo3-deficient BMDCs (Fig. 5d).

To analyze the capacity of BMDCs to enhance T cell survival *in vivo*, CFSE-labeled OTII T cells were transferred into naïve CD45.1 congenic hosts. One day later, wild-type or Foxo3-deficient BMDCs, with or without preloaded OVA peptide, were transferred into the footpads of these mice. After two additional days, *Foxo3*^{Kca} BMDCs induced greater accumulation of OTII T cells in the draining LN, but a similar number of OTII T cell divisions, compared to wild-type DCs (Fig. 5e). Interestingly, *Foxo3*^{Kca} DCs facilitated greater OTII T cell survival, even in the absence of OVA peptide. Together, these data establish that Foxo3-deficient DCs increase antigen-induced T cell population expansion by enhancing survival.

Enhanced IL-6 secretion from *Foxo3*-deficient DCs

To determine if the enhanced T cell survival induced by Foxo3-deficient DCs was due to altered cytokine secretion, wild-type and *Foxo3*^{Kca} mice were infected with LCMV, and

blood plasma cytokine concentrations were measured on various days post-infection. IL-12, IL-17, MCP1, IL-1β, IL-5, IL-10 concentrations were similar in wild-type and *Foxo3*^{Kca} mice (Supplementary Fig. 4a, online), but IL-6 and TNF concentrations were higher in Foxo3-deficient mice (Fig. 6a and Supplementary Fig. 4a, online). To determine if DCs were the source of this abundant IL-6 and TNF, splenic DCs were harvested from mice on day 3 post-infection and were placed in culture for 24 h. *Foxo3*^{Kca} DC supernatants contained significantly higher concentrations of IL-6, TNF, MCP-1, and IFN-γ (Fig. 6b and Supplementary Fig. 4b, online), whereas we detected no differences in IL-10 or IL-12 concentrations. We also observed an increase in IL-6 mRNA expression in *Foxo3*^{Kca} DCs (Fig. 6b).

To determine whether cells other than DCs could be responsible for this increased IL-6 production, T cells, B cells and macrophages were harvested from mice 3 days post LCMV infection and cultured for 24 h. Neither T cells nor B cells produced detectable amounts of IL-6 (data not shown). Macrophages did produce IL-6, although there was no difference depending on *Foxo3* status (data not shown). However, given the increased numbers of macrophages in Foxo3-deficient mice, these cells may contribute to the excess IL-6 production *in vivo*.

We next determined whether BMDCs also produced excess IL-6 in the absence of Foxo3. We detected significantly higher amounts of IL-6 in cultures containing OTII CD4 T cells or OTI CD8 T cells and *Foxo3*^{Kca} BMDCs, compared to those containing T cells and wild-type DCs (Fig. 6c). Confirming the DC-specific nature of this abundant IL-6, RT-PCR revealed a two-fold increase in the amount of IL-6 mRNA in *Foxo3*^{Kca} compared to wild-type BMDCs; the amount of IL-6 mRNA was at least 10-fold greater in BMDCs than in CD4 T cells, and IL-6 mRNA was undetectable in CD8 T cells (Fig. 6d).

In combination with transforming growth factor-β (TGF-β), IL-6 induces differentiation of IL-17-producing T (T_H-17) cells30. Given the results above, we analyzed the balance between T_H-17 and Foxp3$^+$ regulatory T (T_{reg}) cells in Foxo3-deficient mice. The proportion of Foxp3-positive and IL-17-positive CD4 T cells in naïve of LCMV-infected *Foxo3*^{Kca} mice was comparable to those in wild-type littermates (Supplementary Fig. 5, online). We did not detect IL-17 producing cells in the CD8 lineage (data not shown).

To evaluate whether the excess IL-6 produced by Foxo3-deficient DCs is required for their capacity to induce enhanced T cell survival, OTII and P14 T cells were cultured with BMDCs in the presence of an IgG1 isotype control antibody or an IL-6-specific blocking antibody. IL-6 blockade reduced the expansion of T cell populations cultured with *Foxo3*^{Kca} BMDCs to a level resembling that of T cells cultured with wild-type DCs (Fig. 6e). Enumeration of dead cells by 7-AAD staining demonstrated that this reversion was due to a decrease in T cell survival (Fig. 6f). In addition, we determined whether exogenous IL-6 was sufficient to enhance the survival of T cells cultured with wild-type BMDCs. Indeed, we noted a direct correlation between the amount of IL-6 added and the proportion of live T cells in each culture (Fig. 6g)31.

To directly ascertain if IL-6 is responsible for the increased expansion of T cell populations in response to LCMV, we treated mice on days −1 and 4 with 100 μg of anti-IL-6Rα. IL-6Rα blockade substantially reduced the magnitude of LCMV-specific T cell responses in *Foxo3*-deficient mice but did not affect the number of LCMV-specific T cells in wild-type mice (Fig. 6h). Together, these experiments suggest that Foxo3a suppressed IL-6 production in wild-type DCs are restrained from high levels of IL-6 production by Foxo3, and thus, that factors that affect Foxo3 localization and transcriptional activity will influence the magnitude of a T cell-mediated immune response.

Foxo3 acts downstream of CTLA4-induced signals

Stimulation of B7 receptors by cytotoxic T lymphocyte-associated antigen 4 (CTLA-4) promotes Foxo3 nuclear localization and activation of DCs32. As cell surface CTLA-4 expression is induced on activated T cells, we analyzed whether signaling through the B7 receptor inhibits IL-6 production in a Foxo3-dependent manner. Splenic DCs were stimulated with loxoribine, a TLR7 agonist, in the presence of varying amounts of CTLA-4-Ig. IL-6 and TNF production stimulated by loxoribine was strongly inhibited by CTLA-4-Ig in wild-type but not Foxo3-deficient DCs (Fig. 7a). Although treatment with CTLA-4-Ig caused a slight increase in the proportion of dead cells, the same toxicity was observed in wild-type and *Foxo3*^{Kca} splenic DCs (Fig. 7a).

To confirm the involvement of Foxo3 in the inhibition of cytokine production induced by CTLA-4-Ig, we analyzed Foxo3 intracellular localization after loxoribine or CTLA-4-Ig stimulation. Foxo3 remained localized in the cytosol of non-stimulated or loxoribine-treated BMDCs; however, CTLA-4-Ig stimulation strongly promoted the nuclear accumulation of Foxo3 (Fig. 7b)32. Interestingly, signaling through B7 was dominant over TLR7 signals, as DCs treated with both loxoribine and CTLA-4-Ig exhibited Foxo3 nuclear localization. Together, these experiments showed that CTLA-4-Ig treatment profoundly suppressed TLR-induced IL-6 and TNF production in wild-type DCs by promoting Foxo3 nuclear accumulation.

If CTLA-4 signals DCs through B7-1 and B7-2, then blocking CTLA-4 should allow wild-type DCs, like Foxo3-deficient DCs, to enhance T cell survival. To examine this question, TCR transgenic T cells were cultured in the presence of wild-type or *Foxo3*^{Kca} DCs and specific peptides, with or without the addition of blocking anti-CTLA-4. As expected, cultures with *Foxo3*^{Kca} BMDCs contained more viable T cells than cultures with wild-type BMDCs (Fig. 7c). However, the addition of anti-CTLA-4 essentially eliminated the difference in T cell accumulation and viability in these cultures. The results of these experiments are consistent with a role for CTLA-4 in promoting the nuclear localization of Foxo3 and the resulting inhibition of inflammatory cytokines produced by DCs. Previous experiments showed that antibody specific for CTLA4 can enhance an immune response in vivo33,34, although to our knowledge, this has not been demonstrated in an immune response to LCMV. Nonetheless, we were interested to determine whether we could detect a Foxo3-dependent enhanced T cell expansion. Mice were inoculated with 100 μg of CTLA4-specific antibody and 4 h later infected with LCMV. Mice were further inoculated with CTLA4-specific antibody every other day and assayed on day 8. We did not achieve an

enhancement of T cell accumulation in either wildtype or Foxo3-deficient mice (Supplementary Fig. 6 online).

DISCUSSION

In this report, we established an essential role for Foxo3 in modulating the magnitude of antigen-specific T cell immune responses. Foxo3-deficient mice exhibited enhanced T cell proliferation in response to viral infections, an enhancement that was not T cell intrinsic but rather dependent upon the augmented capacity of DCs to sustain T cell viability. Despite the numerous potential targets of Foxo3, including regulators of cell cycle, apoptosis, and reactive oxygen detoxification, *Foxo3* loss-of-function mutation alone had no effect on steady state T cell homeostasis, survival or proliferation. This finding is consistent with our studies showing that Foxo1 is essential for normal T cell homeostasis and self tolerance16 (data not shown). Instead, we revealed a critical DC-intrinsic function for Foxo3 in the control of T cell responses. Foxo3 acted downstream of CTLA-4-induced signals to constrain IL-6 production by DCs. The natural conditions that would override the CTLA-4-mediated nuclear localization of Foxo3 are not presently known; however, a novel immunostimulatory cancer treatment regimen that involves blocking CTLA-4 may act in part through this mechanism35.

These results differ substantially from a previously published characterization of $Foxo3^{Trap}$ mice20. $Foxo3^{Trap}$ mutant mice were derived from an independent insertional mutant ES line obtained from BayGenomics and were backcrossed to the 129 strain for 3 generations. $Foxo3^{Trap}$ mice exhibited spontaneous T cell activation, lymphoproliferation, and organ infiltration associated with constitutive NF-κB activation. In contrast, none of these characteristics were observed in $Foxo3^{-/-}$ or $Foxo3^{Kca}$ mice. T cells isolated from these two strains of mice appeared to be indistinguishable from wild-type T cells in terms of NF-κB activation, expression of activation markers and response to mitogenic stimulation. These results are consistent with previous analyses of $Foxo3^{Kca}$ and $Foxo3^{-/-}$ mice, in that extensive histological analyses did not reveal organ lymphocytic infiltration23,26.

Differences in autoimmunity between mixed C57BL/6 and 129 mouse strains are not uncommon. 129 mice have autoimmunity susceptibility loci, and one of which (*Sle16*) induces humoral autoimmunity in congenic C57BL/6 mice. Several studies have noted modifier genes in the 129 strains that confer enhanced autoimmune disease when analyzing 129 × C57BL/6 mice36–38. $Foxo^{Trap}$ mice are apparently 129 inbred mice without a contribution from C57BL/6, but perhaps a 129 susceptibility locus that modifies the *Foxo3* deficiency is present.

IL-6 is a pleiotropic cytokine that regulates many aspects of the immune system including antibody production, hematopoiesis, inflammation, and, most relevant to this study, T cell survival39. IL-6 rescues resting T cells from apoptosis by inhibiting the downregulation of Bcl-2 in a dose dependent manner40, and IL-6 increases survival of antigen-stimulated T cells31. Consistent with this observation, we noted higher Bcl-2 and Bcl-xL expression in T cells from LCMV-infected $Foxo3^{Kca}$ mice compared to wild-type mice. In addition, the division rate of T cells stimulated with $Foxo3^{Kca}$ DCs was not altered compared to T cells

stimulated with wild-type DCs; rather the effect was manifested as increased T cell survival. Moreover, *Foxo3*^{Kca} DCs sustained T cell viability both *in vitro* and *in vivo* even in the absence of specific peptide suggesting that enhanced T cell survival induced by IL-6 is not restricted to TCR-engaged T cells. Interestingly, IL-6-specific blocking antibody did not affect wild-type T cell viability *in vitro*, nor did it decrease T cell accumulation *in vivo*. This observation implies that, under the conditions tested, the amount of IL-6 produced by wild-type DCs is not sufficient to affect T cell viability. We are interested to know whether immune responses to other agents are sensitive to IL-6 concentrations, and in those infections, whether CTLA-4, T_{reg} cells, and Foxo3 affect the magnitude and dynamics of the T cell response.

CTLA-4 acts as a counterbalance to CD28 costimulation by antagonizing TCR signals in activated T cells and promoting tolerance41. CTLA-4 is also expressed on T_{reg} cells, and is essential for their effectiveness42. CTLA-4 can also modify immune cell function by triggering 'reverse signaling' through B7 receptors; these signals promote the DC production of stimulatory and/or suppressive mediators21. Reverse signals through B7 also activate the immunosuppressive pathway of tryptophan catabolism in plasmacytoid DCs involving indoleamine 2,3-dioxygenase (IDO)43. Foxo3 has a role in the IDO pathway in pDCs, as CTLA-4–Ig leads to Foxo3 nuclear accumulation and superoxide dismutase 2 (SOD2) expression32. As IDO induces T cell death through the generation of kinurenin and tryptophan privation43, we speculated that a potential IDO defect in *Foxo3*^{Kca} DCs could explain the increased T cell survival; however, the addition of 1-methyl-d-tryptophan (1-MT) IDO inhibitor did not enhance T cell survival in cultures containing wild-type or *Foxo3*^{Kca} BMDCs (data not shown). Moreover, IDO is mainly expressed by plasmacytoid and CD8α^+ DC subsets22 and low or no IDO protein is detected in resting DCs derived from BM44. Presumably, CTLA-4 expressed on T_{reg} cells constitutes the major B7 stimulatory ligand, but the possibility that activated T cells or other cells contribute to B7 ligation *in vivo* has not been studied. In addition, the relative contribution of each CTLA-4-mediated suppressive mechanism to the regulation of immune responses to differ infectious agents is not well understood.

Altogether, these experiments indicate that nuclear-localized Foxo3 functions in DCs to inhibit the production of inflammatory cytokines that would otherwise be activated in response to infection. We deduce that the IL-6-induced T cell survival observed in *Foxo3*^{Kca} mice results from an inability of *Foxo3*-deficient DCs to shut down cytokine production in response to CTLA-4 signals. Conditions that alter the activity of Foxo3 such as stress, growth factors or nutrients would be expected to substantially influence the activity of DCs and perhaps macrophages, and such conditions might be expected to alter the outcome of responses to infectious agents.

METHODS

Mice

C57BL/6, C57BL/6-CD45.1, P14, OTI and OTII were maintained in specific pathogen-free conditions at UCSD. C57BL/6 mice lacking *Foxo3* were generated using embryonic stem (ES) cell clones from the OmniBank(R) ES cell library of randomly targeted cell lines

(Lexicon Genetics) 23. These mice (Foxo3$^{Gt(VICTR20)1Kca}$ abbreviated *Foxo3*^{Kca}) were backcrossed to C57BL/6J for 12 generations, and were then intercrossed to generate congenic C57BL/6 *Foxo3*^{Kca} mice. Conditionally targeted *Foxo*$^{L/L}$ mice were produced in FVB ES cells, and the *loxP*-flanked allele deleted by breeding with EIIa-Cre transgenic male mice26. Offspring with a complete excision were bred to exclude EIIa-Cre, and these mice are designated *Foxo3*$^{-/-}$ 26. TCR transgenic mice with a *Foxo3*-null genotype were produced by breeding C57BL/6 *Foxo3*^{Kca} mice with either P14 or OTII mice. All procedures were approved by the UC San Diego Institutional Animal Care and Use Committee.

Virus infection and analysis

Six- to twelve-week-old *Foxo3*^{Kca} mice or wild-type littermates were infected with 2×10^5 PFU of LCMV Armstrong in 0.2 ml of PBS by intraperitoneal injection. Alternatively, mice were infected with 10^5 PFC of VSV^{45} expressing OVA (VSV-OVA) (provided by Dr. L. Lefrançois, University of Connecticut Health Center). At the indicated time points, spleens were harvested from LCMV infected or uninfected control mice and splenocytes were stimulated with gp33 or gp61 peptide (Genemed Synthesis) and 1 μg/ml brefeldin A (Golgistop; BD PharMingen). After 5 h of stimulation, cells were stained for intracellular IFN-γ. For the transfer experiments, CD45.2 congenic wild-type P14 or *Foxo3*^{Kca} P14 T cells (2×10^4) were injected intravenously into CD45.1 wild-type hosts, which were infected with LCMV 24 h later. Conversely, CD45.1 congenic wild-type P14 T cells were transferred into congenic CD45.2 wild-type littermate or *Foxo3*^{Kca} mice. The number of P14 T cells in the spleen was assessed at day 8 after LCMV infection. VSV infections were carried identically except T cells from CD45.2 OTI mice were transferred. For the BM chimera experiments, congenic CD45.1 recipient mice were lethally irradiated (1,200 Rad) and injected intravenously with 2×10^6 BM cells from wild-type littermate or *Foxo3*^{Kca} donor mice (both CD45.2). After 2 months, the reconstitution of peripheral blood lymphocytes was over 90%. These radiation chimeras were then infected with LCMV and the magnitude of the LCMV response was assessed at day 8 post-infection. For antibody blockade of IL-6Rα, wild-type or Foxo3-deficient mice were innoculated intraperitoneally with 100 μg of anti- IL-6Rα (purified anti-mouse/rat CD126, BioLegend) on day −1 and day 4 and infected with LCMV Armstrong at day 0.

Cell isolation and purification

BM cells were isolated by flushing the femur and tibia with RPMI medium (10% fetal bovine serum, 2 mM L-glutamine, 100 U/ml of penicillin, 100 μg/ml of streptomycin and 50 μM beta-mercaptoethanol). Spleens were removed and incubated with collagenase D (1 mg/ml; Roche) for 20 min at 37 °C, and splenocytes were collected by homogenization through a 100 μm tissue strainer. Cells were resuspended in a Tris-ammonium chloride buffer to lyse the red blood cells. For splenic DC purification, cells were first incubated with 2.4G2 hybridoma culture supernatant (anti-mouse FcγRII/III) for 15 min, then with anti-mouse Pan DC microbeads (Miltenyi Biotec) for 20 min, followed by positive selection. The positive fraction was typically more than 95% CD11c$^+$. For T cell purification, splenocytes from P14 or OTII mice were incubated with a mixture of biotinylated anti-B220, anti-CD19,

anti-Gr1, anti-MHCII, anti-DX5, and anti-CD11b (eBioscience) and were negatively selected using strepavidin-coupled microbeads (Miltenyi Biotec) (>95% purity).

BMDC cultures

BM cells were isolated and cultured at 2×10^6 cells/ml in RPMI medium containing 20 ng/ml rmGM-CSF (Peprotech). The rmGM-CSF-supplemented culture was renewed every two days. Cultures were collected on day 8 and $CD11c^+$ cells were selected using microbeads (Miltenyi Biotec), The final population was 98% $CD11c^+$ $CD11b^+$ $B220^-$ DCs.

Flow cytometry

Cells were incubated for 15 min with anti-mouse FcγRII/III and then stained with primary antibodies for 20 min on ice. The following murine mAbs were used: allophycocyanin (APC)- or phycoerythrin (PE)-conjugated anti-CD11c, fluorescein isothiocyanate (FITC)- or PE-conjugated anti-B220, PECy7- or peridin chlorophyll protein (PerCP)-conjugated anti-CD11b, PE-conjugated anti-Ly6C, APC-conjugated anti-CD8α, PE-conjugated anti-CD86, PE-conjugated anti-CD80, FITC-conjugated anti-MHC class I, PE-conjugated anti- MHC class II , PerCP-conjugated anti-CD3, FITC-conjugated anti-Gr-1, PE-conjugated anti-CD19, PE-conjugated anti-CD3, PE-conjugated anti-NK1.1 (all from eBioscience).

T cell proliferation and death assays

For *in vitro* experiments, DCs were purified from wild-type or *Foxo3*^{Kca} mice on day 3 post LCMV infection. DCs were also purified from non-infected mice or were derived from the BM of wild-type or *Foxo3*^{Kca} mice. These DCs were used to stimulated P14 CD8 T cells, OTII CD4 T cells or OTI CD8 T cells (10^5/well) labeled with 1 μM carboxyfluorescein diacetate succinimidyl ester (CFSE; Molecular Probes) in the presence of 0.1 μg/ml of gp33 peptide or 1 μg/ml of $OVA_{323–339}$. Proliferation was analyzed by flow cytometry by measuring CFSE dilution and T cell death was measured by Annexin V and 7-AAD staining. For *in vivo* transfer experiments, CFSE-labeled CD4 T cells purified from OTII mice were injected retro-orbitally into congenic CD45.1 C57BL/6 mice. Wild-type or *Foxo3*^{Kca} BMDCs were pulsed with $OVA_{323–339}$ peptide and injected intradermally after 24 h. Three days later, draining LNs were harvested, stained with APC-conjugated anti-CD4 and PE-conjugated anti-CD45.1 (eBioscience) and analyzed by flow cytometry.

In vitro stimulation of DC and quantitation of cytokine production

2×10^5 sorted DCs were cultured in 96-well round-bottom culture plates (Nunc) and stimulated with medium alone, loxoribine (0.03 mM) (InvivoGen, San Diego, CA) alone or in the presence of recombinant mouse fusion protein consisting of the ectodomain of CTLA-4 linked to the Fc portion of IgG2a (CTLA-4-Ig) at a concentration of 20 or 40 μg/ml (R&D Systems). After culture for 18 h, supernatants were collected, and the cytokine concentration was determined by immunoassay. ELISA kits were used for the detection of TNF or IL-6 (eBioscience; Ready-Set-Go) unless otherwise specified. Cytokines were also measured using Cytokine Bead Array (CBA) (BD Biosciences) or Luminex technology (Invitrogen).

Fluorescence microscopy

DC derived from BM of wild-type or *Foxo3*^{Kca} mice were cultivated on sterile coated Poly-L-Lysine Coverslips (BD BioCoatTM) for 12 h. Cells were fixed in 4% formaldehyde then permeabilized with 0.02% v/v Triton X-100. Coverslips were blocked in PBS containing 5% bovine serum albumin and anti-mouse FcgRII/III for 2 h. Anti-FOXO3 (FKHRL1, Cell Signaling) was added for 1 h, followed by a secondary antibody conjugated to FITC (goat anti-rabbit IgG (Zymex)). For staining of nuclei, 4'-6-Diamidino-2-phenylindole (DAPI) was added at a concentration of 0.04 μg/ml. All cells were visualized using a microscope (Axiovert 200M; Carl Zeiss MicroImaging, Inc.) with a 63× objective. Images were captured with a monochrome digital camera (Axiocam; Carl Zeiss MicroImaging, Inc.) and analyzed with Axiovision software (Carl Zeiss MicroImaging, Inc.).

Semiquantitative RT-PCR

Total RNA was extracted from DCs using Trizol following the manufacturer's instructions (Invitrogen). cDNA was synthesized using SuperScript First-Strand synthesis System for reverse-transcription–polymerase chain reaction (RT-PCR; Invitrogen). *Il6* and Cyclophilin A (*Ppia*) were amplified by PCR using the following primers: *Il6* forward, 5'-acctggagtacatgaagaacaactt -3' and reverse, 5'- ggaagcactcacctcttggt -3'; *Ppia* forward, 5'-caccgtgttcttcgacatc-3' and reverse, 5'- attctgtgaaaggaggaacc-3'.

Immunoblotting

Equal amounts of protein from whole-cell extracts were resolved on 4–12% SDS-PAGE gels (Invitrogen) and transferred to a PVDF membrane (Millipore) using a semi-dry transfer cell (Bio-Rad). Blots were blocked and incubated with the primary antibody at 4°C overnight, followed by 2 h at room temperature with the appropriate HRP-conjugated secondary antibody. Rabbit polyclonal anti-Foxo3a antibody was kindly provided by A. Brunet (Stanford University). Antibodies specific for IκB proteins were purchased from Santa Cruz Biotechnology.

Supplementary Material

Refer to Web version on PubMed Central for supplementary material.

Acknowledgments

A.S.D was supported by a fellowship from Fondation pour la Recherche Médicale. We thank J.P. Allison (Sloan-Kettering Memorial Hospital) and J.A. Bluestone (UC San Francisco) for the generous gifts of CTLA-4-specific blocking antibodies, Anne Brunet for Foxo3-specific antibodies, L. Mack and E. Zuniga for assistance with virus titers, and M. Niwa for the generous use of her microscope facility. R.A.D. is an American Cancer Society Research Professor and supported by the Robert A. and Renee E. Belfer Institute for Innovative Cancer Research and grants from the NCI. This work was supported by funds made available to S.M.H. by the Division of Biological Sciences, UC San Diego.

Abbreviations

DC	dendritic cell
BMDC	Bone marrow derived dendritic cell

IL	Interleukin
LCMV	Lymphocytic Choriomeningitis Virus
CTLA4	Cytotoxic T-Lymphocyte Antigen 4
TLR	Toll like receptor
7-AAD	7-Amino-actinomycinD

References

1. Calnan DR, Brunet A. The FoxO code. Oncogene. 2008; 27:2276–2288. [PubMed: 18391970]
2. Galili N, et al. Fusion of a fork head domain gene to PAX3 in the solid tumour alveolar rhabdomyosarcoma. Nat Genet. 1993; 5:230–235. [PubMed: 8275086]
3. Hillion J, Le Coniat M, Jonveaux P, Berger R, Bernard OA. AF6q21, a novel partner of the MLL gene in t(6;11)(q21;q23), defines a forkhead transcriptional factor subfamily. Blood. 1997; 90:3714–3719. [PubMed: 9345057]
4. Corral J, et al. Acute leukemias of different lineages have similar MLL gene fusions encoding related chimeric proteins resulting from chromosomal translocation. Proc Natl Acad Sci U S A. 1993; 90:8538–8542. [PubMed: 8378328]
5. Jacobs FM, et al. FoxO6, a novel member of the FoxO class of transcription factors with distinct shuttling dynamics. J Biol Chem. 2003; 278:35959–35967. [PubMed: 12857750]
6. Barthel A, Schmoll D, Unterman TG. FoxO proteins in insulin action and metabolism. Trends Endocrinol Metab. 2005; 16:183–189. [PubMed: 15860415]
7. Biggs, WHr; Meisenhelder, J.; Hunter, T.; Cavenee, WK.; Arden, KC. Protein kinase B/Akt-mediated phosphorylation promotes nuclear exclusion of the winged helix transcription factor FKHR1. Proc Natl Acad Sci U S A. 1999; 96:7421–7426. [PubMed: 10377430]
8. Brunet A, et al. Akt promotes cell survival by phosphorylating and inhibiting a Forkhead transcription factor. Cell. 1999; 96:857–868. [PubMed: 10102273]
9. Kops GJ, et al. Direct control of the Forkhead transcription factor AFX by protein kinase B. Nature. 1999; 398:630–634. [PubMed: 10217147]
10. van der Horst A, Burgering BM. Stressing the role of FoxO proteins in lifespan and disease. Nat Rev Mol Cell Biol. 2007; 8:440–450. [PubMed: 17522590]
11. Brunet A, et al. Stress-dependent regulation of FOXO transcription factors by the SIRT1 deacetylase. Science. 2004; 303:2011–2015. [PubMed: 14976264]
12. Motta MC, et al. Mammalian SIRT1 represses forkhead transcription factors. Cell. 2004; 116:551–563. [PubMed: 14980222]
13. Stahl M, et al. The forkhead transcription factor FoxO regulates transcription of p27Kip1 and Bim in response to IL-2. J Immunol. 2002; 168:5024–5031. [PubMed: 11994454]
14. Dijkers PF, et al. Forkhead transcription factor FKHR-L1 modulates cytokine-dependent transcriptional regulation of p27(KIP1). Mol Cell Biol. 2000; 20:9138–9148. [PubMed: 11094066]
15. Barata JT, et al. Activation of PI3K is indispensable for interleukin 7-mediated viability, proliferation, glucose use, and growth of T cell acute lymphoblastic leukemia cells. J Exp Med. 2004; 200:659–669. [PubMed: 15353558]
16. Kerdiles YM, et al. Foxo1 links homing and survival of naive T cells by regulating L-selectin, CCR7 and interleukin 7 receptor. Nat Immunol. 2009; 10:176–184. [PubMed: 19136962]
17. Peng SL. Foxo in the immune system. Oncogene. 2008; 27:2337–2344. [PubMed: 18391975]
18. You H, et al. FOXO3a-dependent regulation of Puma in response to cytokine/growth factor withdrawal. J Exp Med. 2006; 203:1657–1663. [PubMed: 16801400]
19. Riou C, et al. Convergence of TCR and cytokine signaling leads to FOXO3a phosphorylation and drives the survival of CD4+ central memory T cells. J Exp Med. 2007; 204:79–91. [PubMed: 17190839]

20. Lin L, Hron JD, Peng SL. Regulation of NF-kappaB, Th activation, and autoinflammation by the forkhead transcription factor Foxo3a. Immunity. 2004; 21:203–213. [PubMed: 15308101]
21. Orabona C, et al. CD28 induces immunostimulatory signals in dendritic cells via CD80 and CD86. Nat Immunol. 2004; 5:1134–1142. [PubMed: 15467723]
22. Mellor AL, Munn DH. IDO expression by dendritic cells: tolerance and tryptophan catabolism. Nat Rev Immunol. 2004; 4:762–774. [PubMed: 15459668]
23. Hosaka T, et al. Disruption of forkhead transcription factor (FOXO) family members in mice reveals their functional diversification. Proc Natl Acad Sci U S A. 2004; 101:2975–2980. [PubMed: 14978268]
24. Marinkovic D, et al. Foxo3 is required for the regulation of oxidative stress in erythropoiesis. J Clin Invest. 2007; 117:2133–2144. [PubMed: 17671650]
25. Greer EL, Brunet A. FOXO transcription factors at the interface between longevity and tumor suppression. Oncogene. 2005; 24:7410–7425. [PubMed: 16288288]
26. Castrillon DH, Miao L, Kollipara R, Horner JW, DePinho RA. Suppression of ovarian follicle activation in mice by the transcription factor Foxo3a. Science. 2003; 301:215–218. [PubMed: 12855809]
27. Villadangos JA, Schnorrer P. Intrinsic and cooperative antigen-presenting functions of dendritic-cell subsets in vivo. Nat Rev Immunol. 2007; 7:543–555. [PubMed: 17589544]
28. Oldstone MB. Biology and pathogenesis of lymphocytic choriomeningitis virus infection. Curr Top Microbiol Immunol. 2002; 263:83–117. [PubMed: 11987822]
29. Rosas M, et al. IL-5-mediated eosinophil survival requires inhibition of GSK-3 and correlates with beta-catenin relocalization. J Leukoc Biol. 2006; 80:186–195. [PubMed: 16684889]
30. Korn T, Bettelli E, Oukka M, Kuchroo VK. IL-17 and Th17 Cells. Annu Rev Immunol. 2009
31. Rochman I, Paul WE, Ben-Sasson SZ. IL-6 increases primed cell expansion and survival. J Immunol. 2005; 174:4761–4767. [PubMed: 15814701]
32. Fallarino F, et al. CTLA-4-Ig activates forkhead transcription factors and protects dendritic cells from oxidative stress in nonobese diabetic mice. J Exp Med. 2004; 200:1051–1062. [PubMed: 15492127]
33. Leach DR, Krummel MF, Allison JP. Enhancement of antitumor immunity by CTLA-4 blockade. Science. 1996; 271:1734–1736. [PubMed: 8596936]
34. Karandikar NJ, Vanderlugt CL, Walunas TL, Miller SD, Bluestone JA. CTLA-4: a negative regulator of autoimmune disease. J Exp Med. 1996; 184:783–788. [PubMed: 8760834]
35. Zang X, Allison JP. The B7 family and cancer therapy: costimulation and coinhibition. Clin Cancer Res. 2007; 13:5271–5279. [PubMed: 17875755]
36. Botto M, et al. Homozygous C1q deficiency causes glomerulonephritis associated with multiple apoptotic bodies. Nat Genet. 1998; 19:56–59. [PubMed: 9590289]
37. Bickerstaff MC, et al. Serum amyloid P component controls chromatin degradation and prevents antinuclear autoimmunity. Nat Med. 1999; 5:694–697. [PubMed: 10371509]
38. Santiago-Raber ML, et al. Role of cyclin kinase inhibitor p21 in systemic autoimmunity. J Immunol. 2001; 167:4067–4074. [PubMed: 11564828]
39. Kishimoto T. Interleukin-6: from basic science to medicine--40 years in immunology. Annu Rev Immunol. 2005; 23:1–21. [PubMed: 15771564]
40. Teague TK, Marrack P, Kappler JW, Vella AT. IL-6 rescues resting mouse T cells from apoptosis. J Immunol. 1997; 158:5791–5796. [PubMed: 9190930]
41. Keir ME, Sharpe AH. The B7/CD28 costimulatory family in autoimmunity. Immunol Rev. 2005; 204:128–143. [PubMed: 15790355]
42. Wing K, et al. CTLA-4 control over Foxp3+ regulatory T cell function. Science. 2008; 322:271–275. [PubMed: 18845758]
43. Grohmann U, et al. CTLA-4-Ig regulates tryptophan catabolism in vivo. Nat Immunol. 2002; 3:1097–1101. [PubMed: 12368911]
44. Hara T, et al. High-affinity uptake of kynurenine and nitric oxide-mediated inhibition of indoleamine 2,3-dioxygenase in bone marrow-derived myeloid dendritic cells. Immunol Lett. 2008; 116:95–102. [PubMed: 18179826]

45. van Stipdonk MJ, Lemmens EE, Schoenberger SP. Naive CTLs require a single brief period of antigenic stimulation for clonal expansion and differentiation. Nat Immunol. 2001; 2:423–429. [PubMed: 11323696]

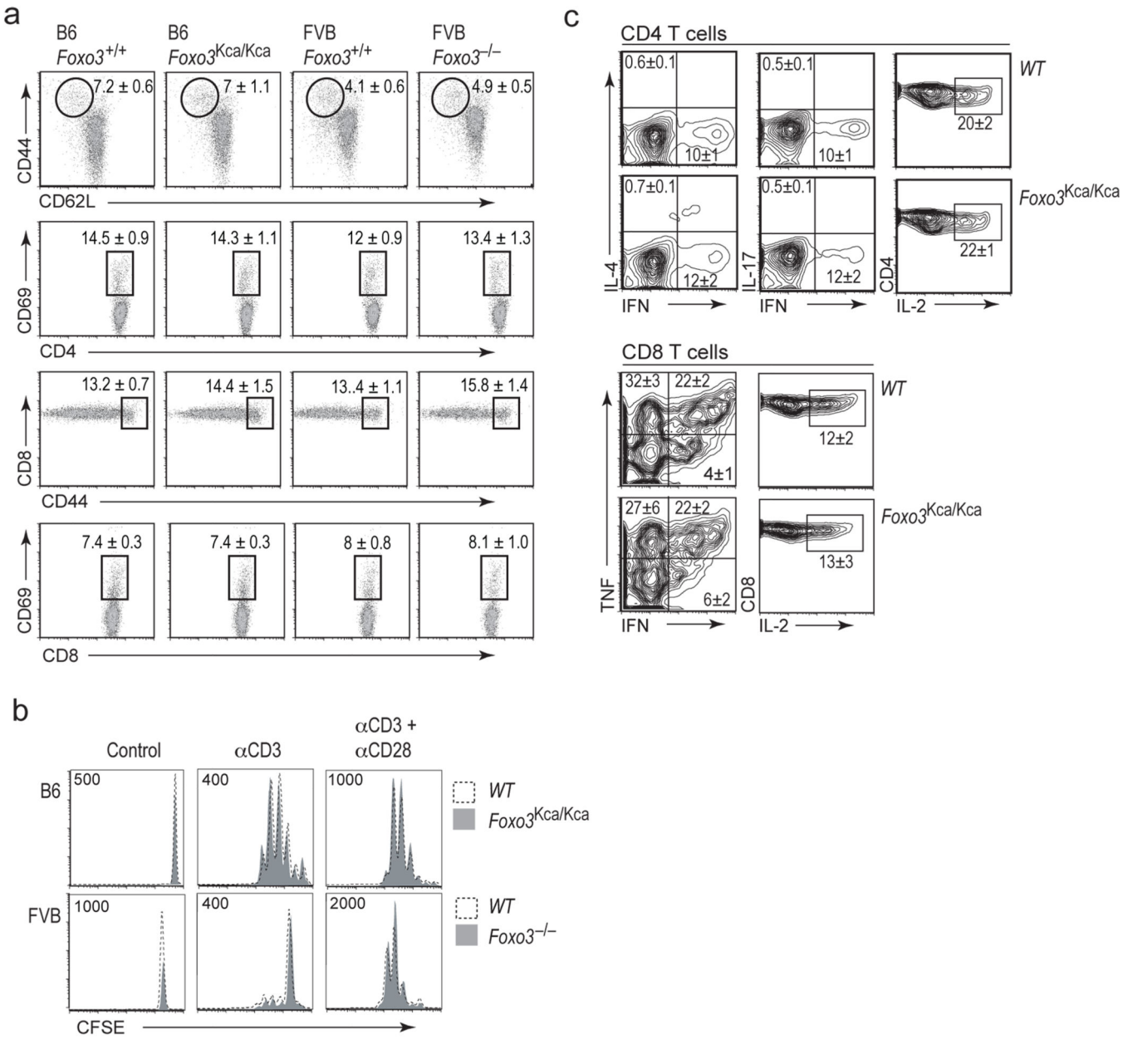

Figure 1.

Foxo3-deficient mice exhibit no spontaneous T cell activation. **(a)** T cells from C57BL/6 *Foxo3Kca*, FVB *Foxo*$^{-/-}$ and their wild-type congenic littermates were analyzed by flow cytometry for CD44, CD62L and CD69 expression. Top panels were gated on CD4 T cells, bottom panels on CD8 T cells. Data show mean ± s.e.m. n = 5–6 mice per genotype analyzed in 5 separate experiments **(b)** CFSE-labeled CD4 T cells from wild-type littermates, *Foxo3*^{Kca} or *Foxo*$^{-/-}$ mice were activated in the presence of anti-CD3 alone or with anti-CD28. Proliferation was assessed by CFSE dilution after 72 h of stimulation. **(c)** Splenocytes from *Foxo3*$^{Kca/Kca}$ mice or wild-type littermates were activated in the presence of PMA and ionomycin for 3 h. Cytokine secretion was analyzed by intracellular staining.

Plots are gated on CD4 (top) or CD8 (bottom) T cells. Similar results were obtained with LN T cells. (n = 6 mice per group). Data are representative of three **(b,c)** independent experiments.

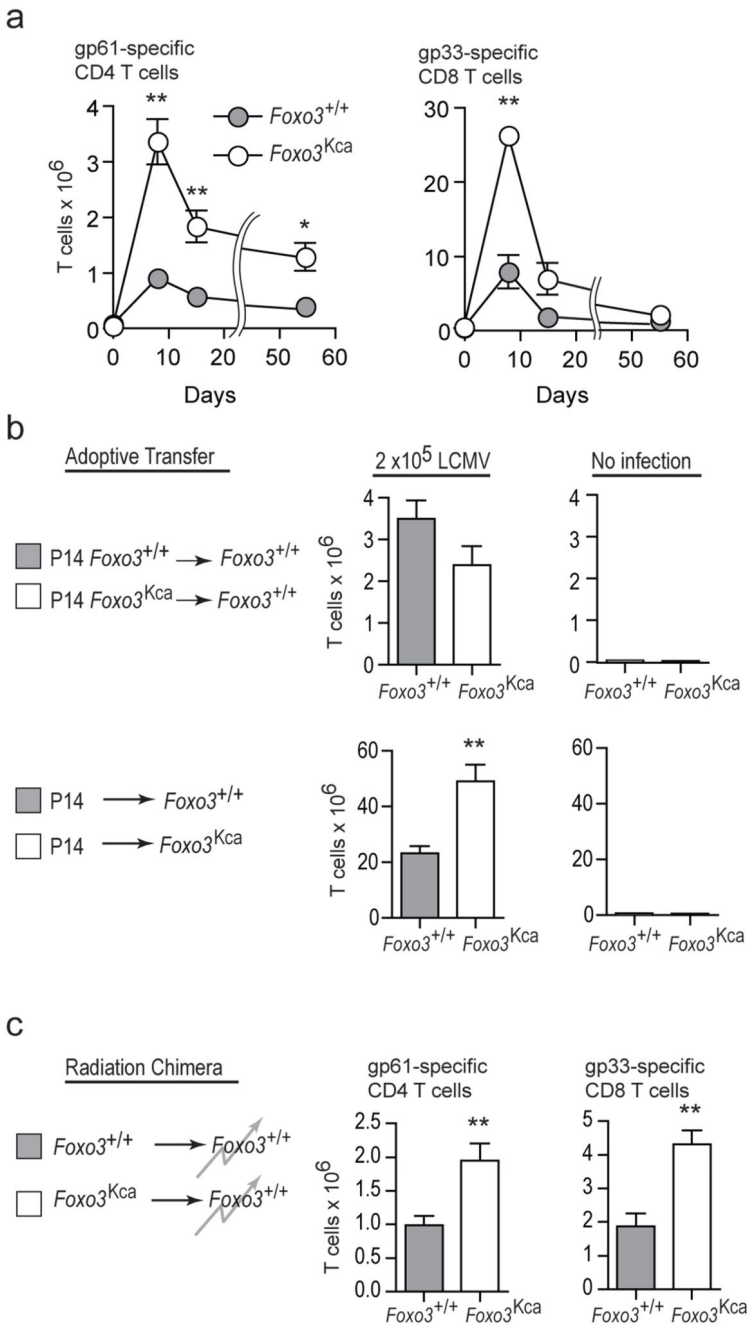

Figure 2.

Foxo3 regulates the magnitude of an LCMV-induced immune response **(a)** Wild-type littermate or *Foxo3*^{Kca} mice were infected with LCMV Armstrong (2×10^5 PFU/mice). The CD4 and CD8 T cell response to LCMV was analyzed following restimulation with gp61 or gp33 peptides, respectively, and intracellular staining for IFN-γ. **(b)** CD45.2 congenic wild-type or *Foxo3*^{Kca} P14 T cells were transferred into CD45.1 wild-type hosts (top) and CD45.1 congenic wildtype P14 T cells were transferred into CD45.2 wild-type or CD45.2 *Foxo3*^{Kca} mice (bottom). Recipient mice were infected with LCMV or were left uninfected,

and P14 T cells were enumerated using a congenic marker 8 days later. **(c)** Lethally irradiated CD45.1 wild-type mice were reconstituted with CD45.2 congenic wild-type or *Foxo3*^{Kca} BM. Eight weeks later, mice were infected with LCMV and virus-specific T cells were enumerated by specific peptide restimulation and intracellular IFN-γ staining. Data are representative of four **(a)** or two **(b–c)** independent experiments with at least three mice per group. (** denotes $p<0.005$, unpaired two-tailed Student t-Test)

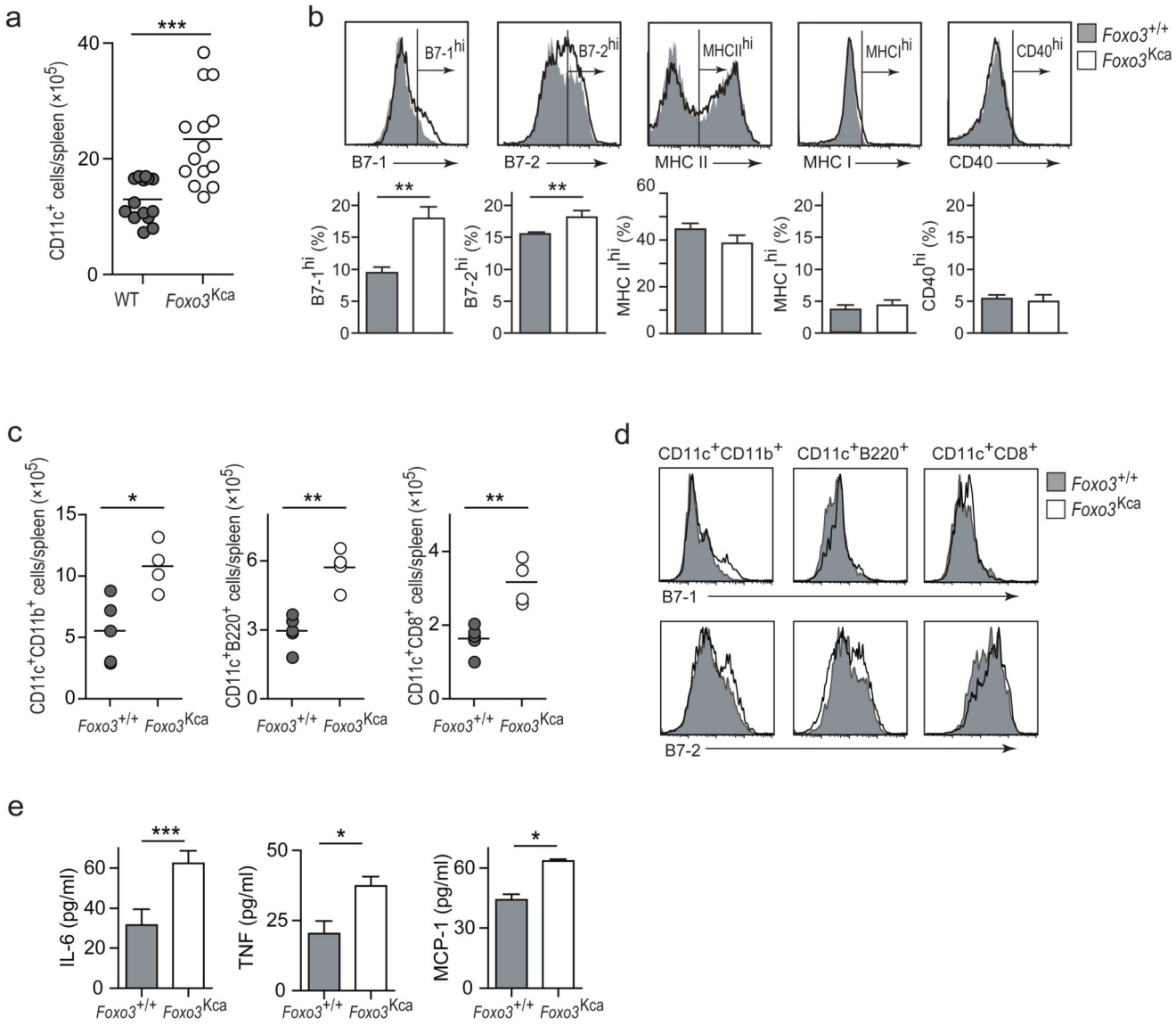

Figure 3.

Increased number and activation of DCs in *Foxo3*^{Kca} mice **(a)** Splenocytes from *Foxo3*^{Kca} and wild-type littermates (n = 10 mice per group) were stained for CD11c expression and the total DC number was calculated. **(b)** CD11c^{+} DCs from naïve *Foxo3*^{Kca} or wild-type littermates (n = 5 mice per group) were stained with antibodies specific for the indicated markers and analyzed by flow cytometry. The accumulation of data is graphed under each histogram **(c)** Absolute numbers of CD11c^{+}CD11b^{+}CD8^{-}; CD11c^{+}CD11b^{-}CD8^{+} and CD11c^{+}B220^{+} DCs in the spleen of *Foxo3*^{Kca} and wild-type littermates was determined (n = 5 mice per group). **(d)** Expression of B7-1 and B7-2 on indicated DC subsets from *Foxo3*^{Kca} and wild-type littermates was measured by flow cytometry. **(e)** Total splenic DCs (CD11c^{+}) were purified from wild-type or *Foxo3*^{Kca} mice and 400,000 cells were cultured for 24 h. Concentrations of IL-6, TNF, MCP-1, IL-10, IFN-γ and IL-12p70 in culture supernatants were measured by CBA. Data are representative of three independent experiments **(a–b)** or

two independent experiments with at least three mice per group **(c–e)**. (* signifies $p<0.01$, ** signifies $p<0.005$, *** signifies $p<0.001$, unpaired two-tailed Student t-Test).

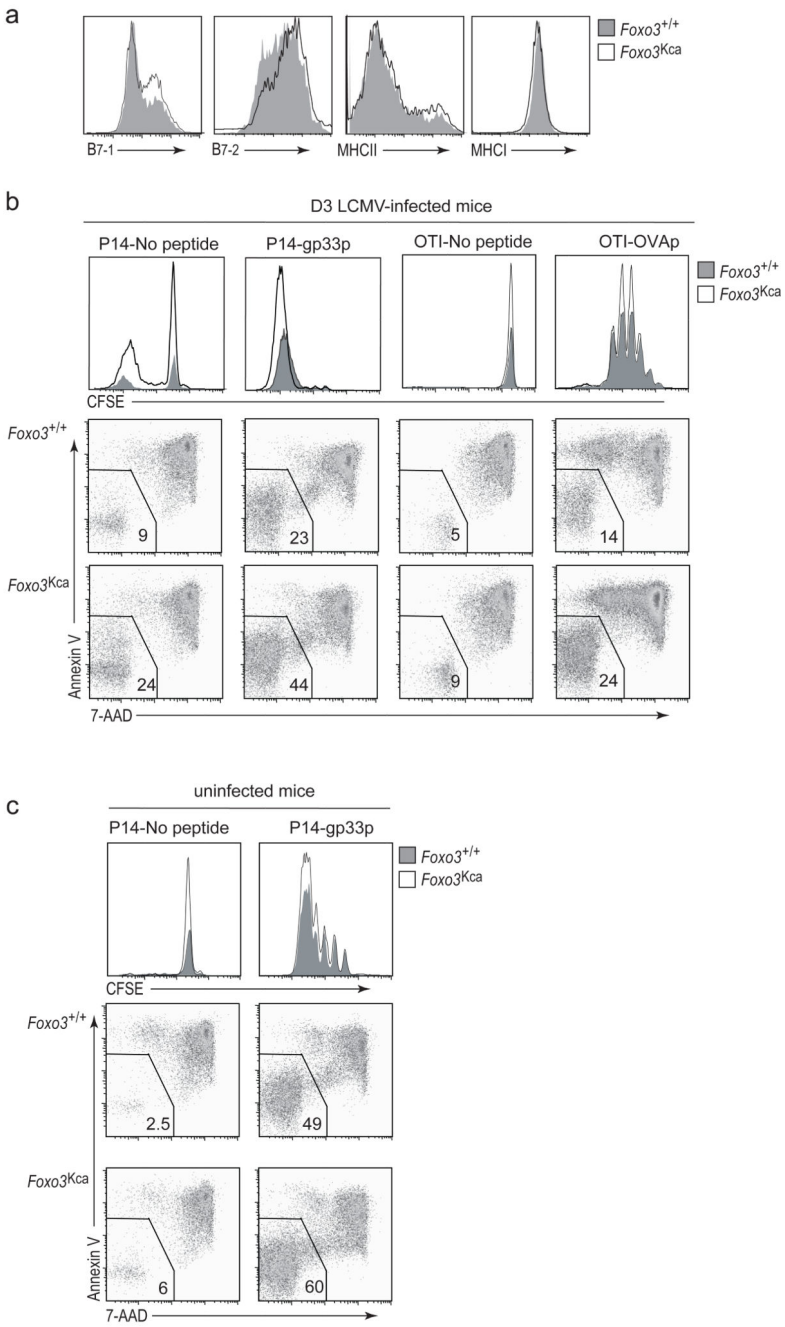

Figure 4.

Increased immunogenicity of LCMV-infected *Foxo3*$^{-}$deficient DCs **(a)** Expression of activation markers on wild-type and *Foxo3*^{Kca} DCs on day 3 post LCMV infection was analyzed by flow cytometry. **(b)** DCs isolated from day 3 LCMV infected *Foxo3*^{Kca} mice or wild-type littermates were used to stimulate CFSE-labeled wildtype P14 CD8 T cells in the presence or absence of gp33 peptide. Bystander proliferation was assessed using CFSE-labeled wildtype OTI CD8 T cells stimulated in the presence or absence of OVA peptide. T cell proliferation was quantified by CFSE dilution and T cell viability was measured by 7-

AAD and Annexin V staining after 3 days of culture. Numbers in dot plots indicate percentage of live CD8 T cells. **(c)** DCs purified from the spleen of uninfected mice were cultured and analyzed as described in **(b)**, and cultured with T cells from P14 mice. Data are representative of two independent experiments with at least three mice per group **(a and c)** or three independent experiments **(b)**.

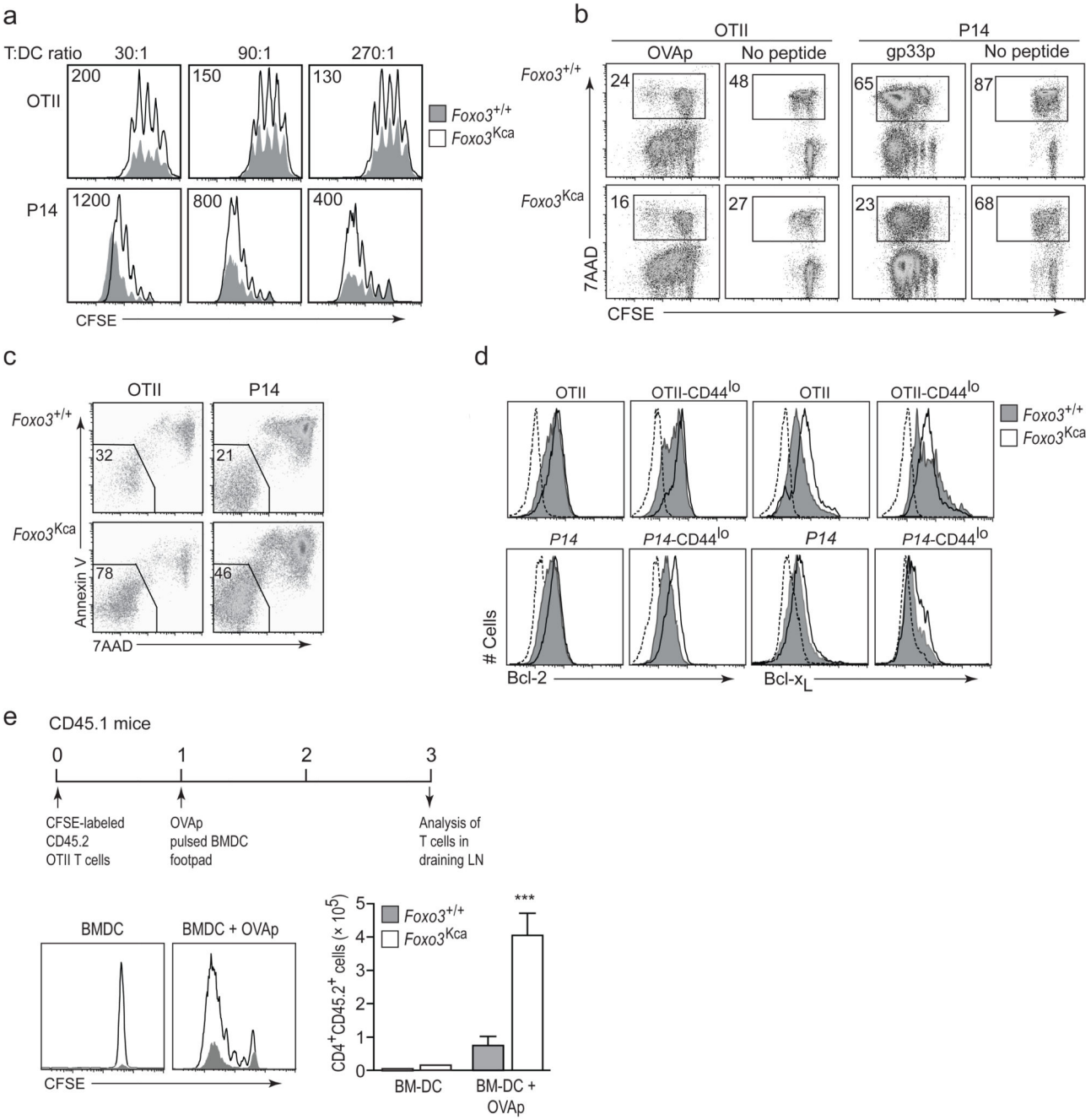

Figure 5.

Enhanced T cell response induced by *Foxo3*^{Kca} BMDCs **(a)** Wild-type OTII CD4 T cells or wild-type P14 CD8 T cells were stimulated at various ratios with wild-type or *Foxo3*^{Kca} BMDCs in the presence of $OVA_{323–239}$ or gp33 peptide, respectively. After 3 days of culture, T cell accumulation was measured by CFSE dilution. **(b)** 1×10^5 OTII or P14 T cells were cultured with 3.3×10^2 wild-type or *Foxo3*^{Kca} BMDCs in the presence or absence of the appropriate peptide. T cell death was assessed by 7-AAD staining. Numbers in dot plots indicate the percentage of 7-AAD$^+$ CD8$^+$ or CD4$^+$ T cells. **(c)** OTII or P14 T cells

were cultured with BMDCs for 3 days in the presence or absence of the appropriate peptide as in **(b)** and stained with 7-AAD and Annexin V. Numbers in dot plots indicate the percentage of viable CD4 or CD8 T cells. **(d)** OTII or P14 T cells were cultured as in **(b)** and the expression of Bcl-2 and Bcl-xL in total T cells or gated $CD44^{lo}$ T cells was analyzed by flow cytometry. The dashed line indicates the isotype control. **(e)** CD4 T cells purified from wild-type CD45.2 OTII mice were labeled with CFSE and injected intravenously into CD45.1 recipient mice. $OVA_{323–239}$ (OVAp) pulsed or unpulsed BMDC from wild-type littermates or $Foxo3^{Kca}$ mice were then injected subcutaneously into the footpad of the same recipient mice. Three days later, CD4 CD45.1 cells in the draining LNs were enumerated and proliferation analyzed by CFSE dilution. Graphs show mean ± sem. $n = 4$ mice per group). Data are representative of at least six independent experiments **(a–b)**, two independent experiments **(c–d)**, or three independent experiments **(e)**.

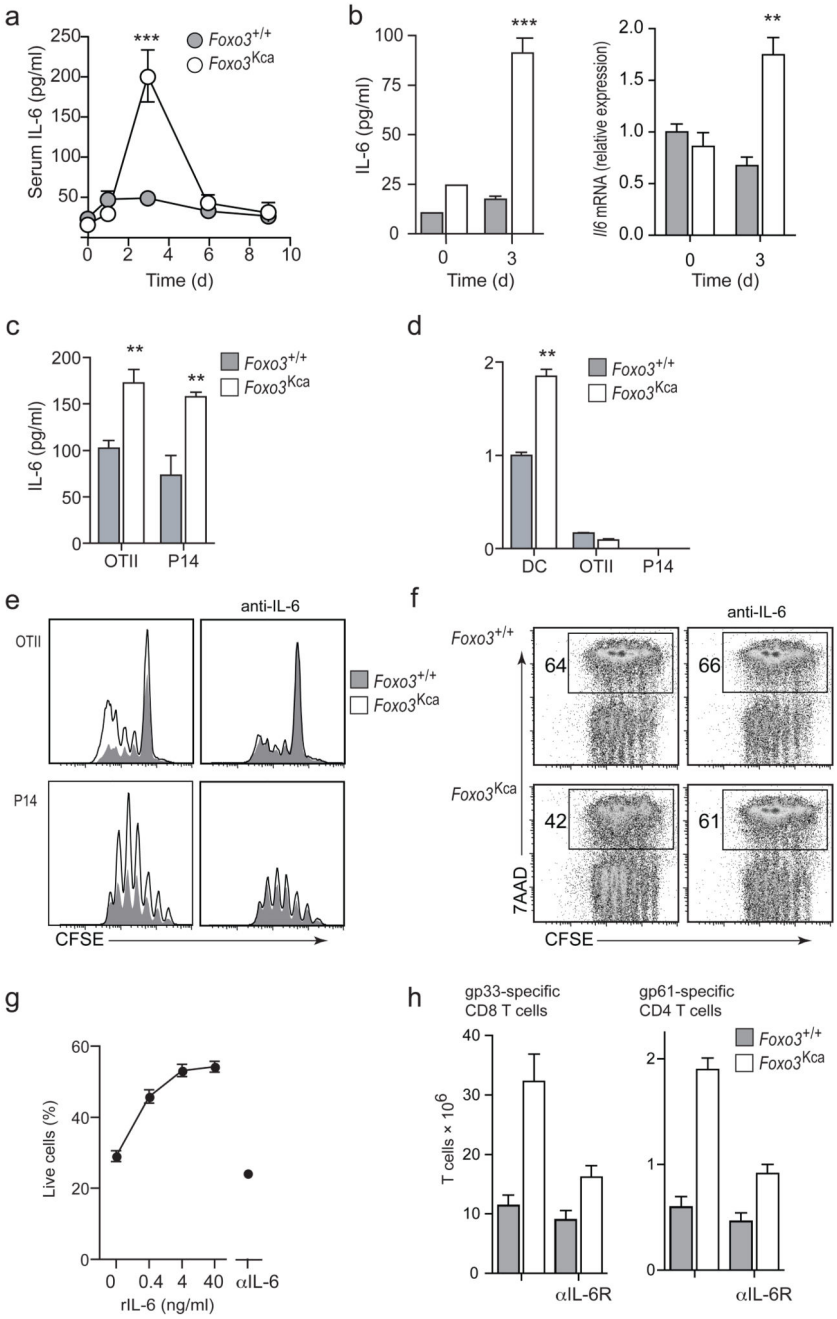

Figure 6.

IL-6 synthesis by Foxo3-deficient DCs is involved in enhanced T cell survival. **(a)** Plasma from wild-type or *Foxo3*^{Kca} mice (n = 4 mice per group) was collected on the indicated days post LCMV infection. The amount of IL-6 in the plasma was measured by CBA. **(b)** DCs (CD11c^{+}) were purified from wild-type or *Foxo3*^{Kca} uninfected mice or 3 days post LCMV infection (n = 4 mice per group). 200,000 cells were cultured for 24 h, and secreted IL-6 was measured using CBA. The relative expression of *Il6* mRNA was measured by rtPCR **(c)** Wild-type OTII or P14 T cells were cultured in the presence of $OVA_{323–339}$ or gp33

peptide-loaded wild-type or *Foxo3*^{Kca} BMDCs as described in Fig. 5. IL-6 concentrations in the supernatants were assessed by ELISA. **(d)** BMDC, OTII and P14 T cells were purified after 2 days of culture as described in **(c)**. *Il6* mRNA was measured by RT-PCR and was normalized to *Gapdh* mRNA. **(e,f)** BMDCs generated from wild-type or *Foxo3*^{Kca} mice were pulsed with $OVA_{323–339}$ or gp33 peptide and used to activate wild-type OTII or P14 T cells, respectively, in the presence of an IgG1 isotype control antibody or IL6-specific blocking antibody (10 μg/ml). After 3 days of culture, T cell accumulation was measured by CFSE dilution and T cell death was measured by 7-AAD staining. **(g)** BMDC generated from wild-type mice were used to stimulate P14 T cells in the presence of increasing amounts of recombinant IL-6. After 3 days of culture, T cell death was assessed by 7-AAD staining. **(h)** Wild-type littermate or *Foxo3*^{Kca} mice (n = 4 mice per group) were treated on day −1 and day 4 with 100 μg of anti IL-6Rα and infected at day 0 with LCMV Armstrong. The LCMV-specific T cell response was analyzed on day 8 post-infection by enumeration of CD8 and CD4 T cells producing IFN-γ after restimulation with gp33 and gp61, respectively. Data are representative of three independent experiments **(a–f)** or two independent experiments **(g–h)**.

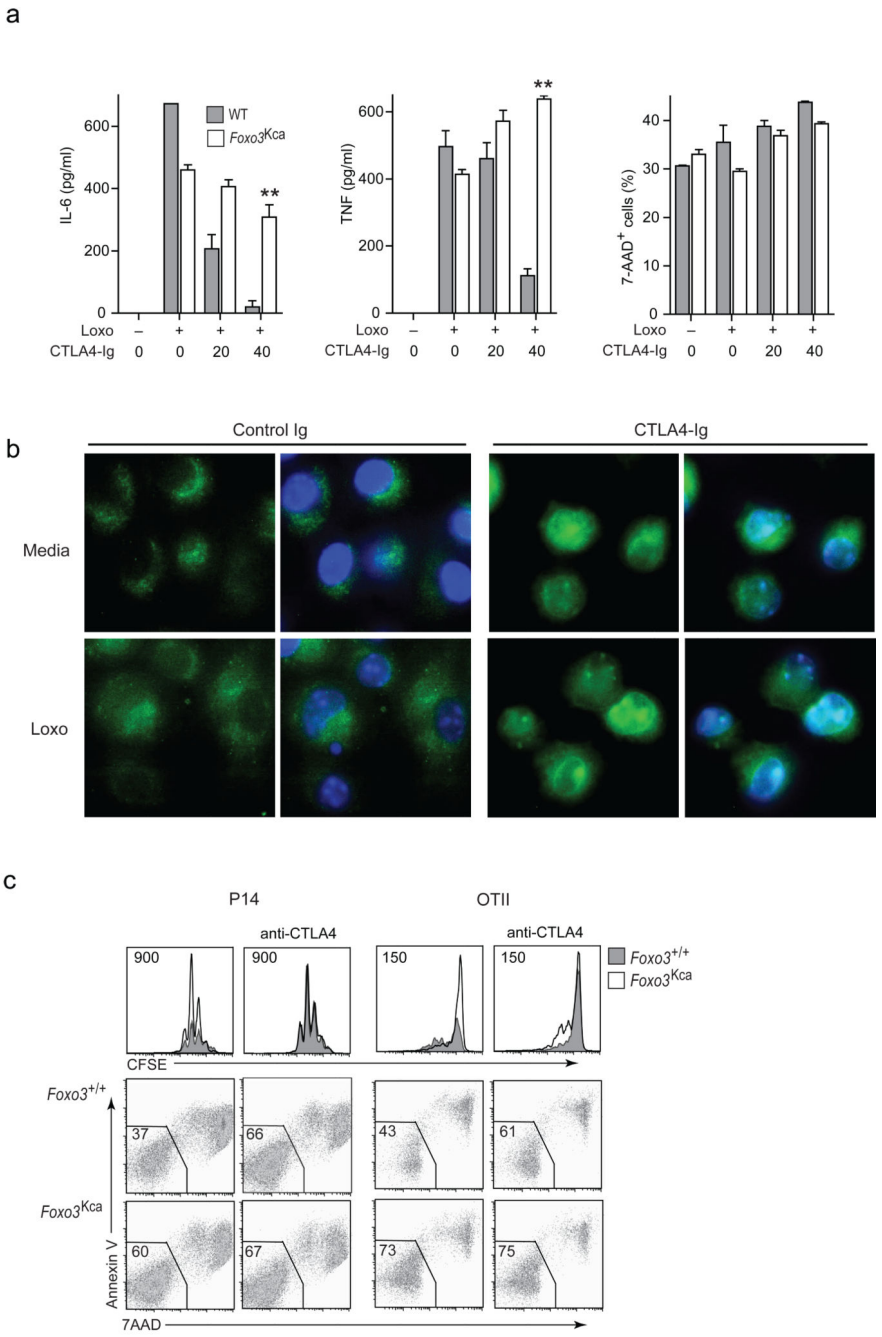

Figure 7.

IL-6 and TNF production by stimulated DCs is inhibited by CTLA-4-Ig stimulation in a Foxo3-dependent manner. **(a)** 2×10^5 DCs purified from the spleen of wild-type littermate or *Foxo3*^{Kca} mice were stimulated for 18 h with or without loxoribine along with increasing amounts of CTLA-4-Ig (μg/ml). IL-6 and TNF concentrations in the supernatants were assessed by immunoassay. DC viability was determined by 7-AAD staining **(b)** Foxo3 localization (green) was assessed by immunoflorescence after 18 h of stimulation with CTLA-4-Ig and/or loxoribine. Dapi, blue. **(c)** 1×10^5 OTII CD4 T cells or P14 CD8 T cells

were cultured with 3.3×10^2 wild-type or *Foxo3*^{Kca} BMDCs in the presence or absence of the appropriate peptide. 50 μg/ml of anti-CTLA-4 (9D9) was added to the culture. After 3 days, T cell accumulation was measured by CFSE dilution, and T cell death was assessed by 7-AAD and Annexin V staining. Numbers in dot plots indicate percentages of live CD4 or CD8 T cells. Data are representative of at least two independent experiments.

Table 1

Leukocyte subsets from *Foxo3*-deficient mice

Spleen	**B6**	**B6**	**FVB**	**FVB**
	Foxo3$^{+/+}$	*Foxo3*$^{Kca/Kca}$	*Foxo3*$^{+/+}$	*Foxo3*$^{-/-}$
CD4	15.0 ± 2.0‡	17.3 ± 1.6	29.3 ± 5.1	31.0 ± 5.9
CD8	13.4 ± 3.5	9.7 ± 1.3	13.0 ± 2.2	14.9 ± 1.9
B220	46.9 ± 6.7	51.7 ± 9.2	58.2 ± 9.7	56.3 ± 12.1
Gr-1^{hi}CD11b^{hi}	1.4 ± 0.2	6.0 ± 1.1*	2.0 ± 0.2	5.4 ± 0.3*
Lymph Nodes				
CD4	10.3 ± 1.4	9.4 ± 1.2	11.0 ± 2.5	12.8 ± 2.4
CD8	7.9 ± 1.0	7.3 ±0.7	5.5 ±1.2	7.0 ±1.4
B220	13.8 ± 1.4	12.4 ± 1.1	4.0 ± 1.2	3.6 ± 0.7

‡The number of cells × 10^6 ± s. e. m., n = 5–6 mice per group.

* indicates significance between wild-type and *Foxo3*-deficient mice P< 0.001 (t-test two sample assuming equal variances).